Supporting Information

Acidified Naphthalene Diimide Covalent Organic Frameworks with Superior Proton Conduction for Solid-State Proton Batteries

Lin-Lin Wang,[a] Xiao-Qin Ni,[a] Ya-Juan Han,[a] Jin Zhang,[a] Hong-Bin Luo,[a] Qiao Qiao,[*a,b] Yu-Ping Wu,[b,c] and Xiao-Ming Ren[*a,d]

[a] College of Chemistry and Molecular Engineering, Nanjing Tech University, Nanjing 211816, P. R. China

[b] School of Energy Science and Engineering, Nanjing Tech University, Nanjing 211816, P. R. China

[c] Key Lab of Energy Thermal Conversion and Control of the Ministry of Education, School of Energy and Environment, Southeast University, Nanjing, 210096, China.

[d] State Key Laboratory of Coordination Chemistry, Nanjing University, Nanjing 210023, P. R. China

Email: qqiao@njtech.edu.cn (QQ); xmren@njtech.edu.cn (XMR)

Table of Contents

1. Experimental section

1.1 Materials and chemicals

1,2-dichlorobenzene ($C_6H_4Cl_2$), hexonecyclohexane octahydrate ($C_6O_6 \cdot 8H_2O$), polytetrafluoroethylene concentrate (PTFE, 60 wt%), potassium chloride (KCl), nitric acid (HNO_3), nickel (II) chloride hexahydrate ($NiCl_2 \cdot 6H_2O$) and potassium (II) hexacanocyanoferrate trihydrate ($K_4Fe(CN)_6 \cdot 3H_2O$) were purchased from Aladdin, 1,4,5,8-naphthalene tetramethyl anhydride ($C_{14}H_4O_6$), imidazole ($C_3H_4N_2$) and 85% phosphoric acid (H_3PO_4) were purchased from Shanghai Maclin Biochemical Technology Co., LTD. 80% hydrazine hydrate ($H_4N_2 \cdot H_2O$) and acetone (C_3H_6O) were purchased from Yonghua Chemical Technology Co., LTD. N,N-dimethylformamide (C_3H_7NO), hydrochloric acid (HCl), acetic acid (CH_3COOH), tetrahydrofuran (C_4H_8O) and ethanol (CH_3CH_2OH) were supplied by China Sinopharm Chemical Reagent Co., LTD. Ammonium molybdate tetrahydrate ($(NH_4)_6MoO_{24} \cdot 4H_2O$) was purchased from Kehua Research Institute. Carbon black (super P) was purchased from MJS Energy Technology, are reagent grade, without further purification. The Mill-Q filtration system produced deionized water (H_2O).

1.2 Synthesis of 2,7-diaminobenzo[lmn][3,8]phenanthroline-1,3,6,8(2H,7H)-tetraone (NDI-NH_2)

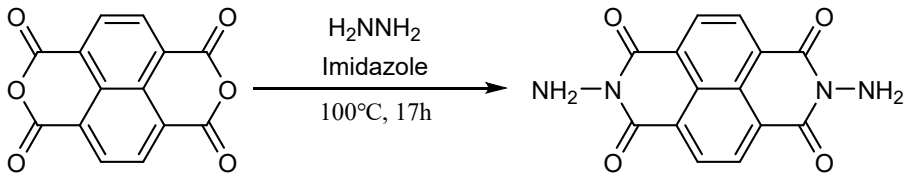

NTCDA **NDI-NH_2**

NDI-NH_2 was synthesized according to the synthetic route with slight changes.[1] 1,4,5,8-Naphthalenetetracarboxylic dianhydride (NTCDA, 2.7 g, 10 mmol) was dissolved in imidazole (25 g). After the imidazole had completely melted upon heating, hydrazine hydrate (2.5 g) was added to the solution. The mixture was stirred at 100 ℃ for 17 hours. After cooling to room temperature, 2 M HCl (1 L) was added to the reaction mixture. The resulting precipitate was collected by filtration and washed sequentially with 2 M HCl and distilled water. The yellow NDI-NH_2 powder was obtained after drying in a vacuum at 110 ℃ for 12 hours, yielding 80%.

1.3 Synthesis of PNDI-COF and PA@PNDI-COF

1,4,5,8-naphthalene diimide derivates 2,7-diaminobenzo[lmn][3,8]phenanthroline-1,3,6,8(2H,7H)-tetraone (NDI-NH_2, 89 mg, 0.3 mmol), hexaketocyclohexane octahydrate (HKH, 17 mg, 0.1 mmol), N,N-dimethylformamide (DMF, 2 mL), 1,2-dichlorobenzene (o-DCB, 2mL) and 6 M HAc (0.2 mL) were added to a 10 mL Schlenk tube. After magnetic stirring at 120℃ argon for 72 hours, brown precipitates were obtained and washed with DMF and acetone in turn, then purified by Soxhlet extraction for 24 hours with tetrahydrofuran (THF) as solvent. The powder was collected and dried in vacuum at 80 °C for 12 hours to afford dark-brown PNDI-COF powder with a 75% yield. PA@PNDI-COF was synthesized by mechanically grinding PNDI-COF with phosphoric acid (PA). Specifically, 100 mg of PNDI-COF was combined with 120 μL of PA and ground at 1600 rpm for 200 minutes via ball-milling method, and dried at 60℃ for 2 hours before membrane preparation.

1.4 PA@PNDI-COF/PTFE membrane preparation

PA@PNDI-COF was mixed with PTFE (25 wt%) as the binder to prepare PA@PNDI-COF/PTFE membrane. Firstly, 55.6 mg PTFE concentration dispersion (60 wt%) and 300 mg PA@PNDI-COF were mixed, and mechanically milled to give uniform mixture, and further rolled into a membrane with the thickness of ~0.1 mm, finally dried in an oven at 80 ℃.

1.5 Synthesis of α-MoO_3 and $K_2NiFe(CN)_6$ (Ni-PBA)

α-MoO_3 was synthesized via a modified hydrothermal method.[2] 1.0 g of $(NH_4)_6MoO_{24}$•$4H_2O$ was dissolved in 30 mL deionized water, followed by the addition of 10 mL of a 3 M HNO_3 solution. After stirring for 20 minutes, the resulting solution was transferred into a Teflon-lined stainless-steel autoclave and heated at 180 ℃ for 24 hours. The white precipitate obtained after the reaction was collected by centrifugation and washed with deionized water and ethanol. The product was subsequently dried under vacuum at 60 ℃ for 24 hours.

The synthesis of Ni-PBA was based on a co-precipitation reaction in an aqueous solution.[3] The solution A was created by dissolving 3 mmol $K_4Fe(CN)_6 \cdot 3H_2O$ and 0.16

mol KCl in 150 mL of deionized water while stirring. Under vigorous stirring at 70°C, the green $NiCl_2 \cdot 6H_2O$ solution (150 mL, 0.04 mol L^{-1}) was added dropwise to solution A. The gray-green precipitates were centrifuged many times with deionized water and ethanol after the initial 6-hour reaction, and they were then vacuum-dried for 24 hours at 60 °C.

1.6 Electrode preparation and proton battery assembly

The preparation of the Ni-PBA electrodes involved combining the active material, conductive additive (super P), and binder (PTFE) in ethanol solvent at a mass ratio of 6:3:1 for Ni-PBA. After drying, the mixtures were pressed into a thin membrane with an active mass loading of ~2 mg cm^{-2} and dried at 60 ℃ overnight in vacuum oven. The obtained membrane was pressed on a titanium mesh. The preparation method of the α-MoO_3 film anode is the same as that of the Ni-PBA film cathode, except that the mass ratio of α-MoO_3: carbon black: PTFE is 7:2:1. The specific capacity calculated based on cathode weight. The pouch cell was assembled by using Ni-PBA and MoO_3 electrodes as the cathode and the anode, respectively. The electrolyte used were H_2SO_4 (0.1 M and 1 M) and PA@PNDI-COF/PTFE membrane, respectively.

1.7 Electrochemical characterization

Cycling voltammetry (CV) and Linear sweep voltammetry (LSV) were performed on a Gamry 600+ electrochemical workstation. Linear sweep voltammetry (LSV) test used platinum electrode as working electrode and counter electrode, saturated calomel electrode (SCE) as reference electrode. Impedance spectra were recorded using a Gamary 600+ electrochemical workstation with conventional two-electrode method, the alternating current (AC) frequencies range from 1 to 1×10^6 Hz with 10 mV signal amplitude. The as-synthesized sample was pressed into a disk with a diameter of 7 mm at a pressure of about 15 MPa for 5 min and formed into a disc with a thickness of 1.2 mm for PNDI-COF. The disc was sandwiched between two platinum electrodes and fixed with a rubber band to measure the impedance spectrum. 180 mg PA@PNDI-COF was filled into a polyether ether ketone (PEEK) tube 10 mm in diameter, and the electrodes of two gold flakes were put into the tube from the both ends, then the sample

was compressed into a pellet with a thickness of ~2.0 mm by applying pressure. The formula is σ = L/RS. Where R is the resistance, L is the thickness of the disc or film, and S is the cross-sectional area of the disc or platinum electrode, the proton conductivity (σ) is calculated. The activation energy (E_a) was calculated from the Arrhenius equation $\sigma = \sigma_0 \exp\left(\frac{-E_a}{k_B T}\right)$,where σ_0, k_B, and T denote the pre-exponential factor, Boltzmann constant, and temperature, respectively. The LAND CT2001 battery testing system was employed to perform Galvanostatic Charge-Discharge (GCD) and Galvanostatic Intermittent Titration Technique (GITT) tests on solid-state proton batteries, and the voltage window range was 0-1.4V. The specific capacity of the proton battery was calculated according to Ni-PBA cathode.

1.8 General methods

Powder X-ray diffraction (PXRD) was collected on a Rigaku MiniFlex 600X with Cu-kα radiation (λ=1.5404 Å). Fourier-transform infrared (FT-IR) spectra was recorded on the Nicolet iS (4000-400 cm^{-1}) spectrophotometer. Thermogravimetric (TG) measurements were carried out by a Netzsch STA 449f5 instrument with a temperature rise rate of 10 ℃ min^{-1} and a temperature of 25-800 ℃. ^1H NMR spectra were recorded on a Bruker Avance III HD 400 MHz NMR spectrometer. N_2 adsorption/desorption isotherm at 77 K was performed using a Micromeritics ASAP 2460 analyzer. X-ray photoelectron spectroscopy (XPS) analyses were conducted on a PHI5000 VersaProbe using Al-Kα as X-ray source. Energy dispersive spectroscopy (EDS) and scanning electron microscopy (SEM) were characterized on the ZEISS GeminiSEM 300 field emission scanning electron microscope. The transmission electron microscope (TEM) images were obtained by the FEI Talos F200X G2 field transmission electron microscope. Chronoamperometry measurements were conducted on Gamry 600+ electrochemical workstation to assess PA@PNDI-COF/PTFE membrane electronic conductivity. The applied DC voltage was set at 0.1 V. The sample has dimensions of 0.1 mm in thickness and 10.0 mm in diameter. Electron current was determined by

fitting current-time plots to the equation of $I = I_0 + A_0 exp(-\frac{t}{t_0})$, in which I is the total current, I_0 is the electron current, A_0 and t_0 are the constants.

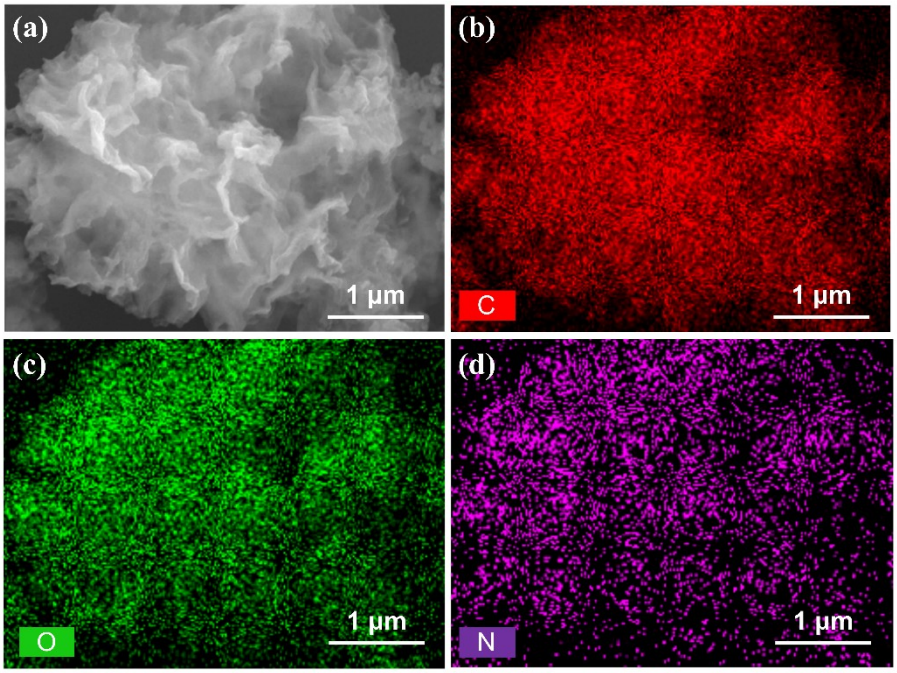

Figure S1. (a) SEM image and (b-d) EDS mapping of PNDI-COF.

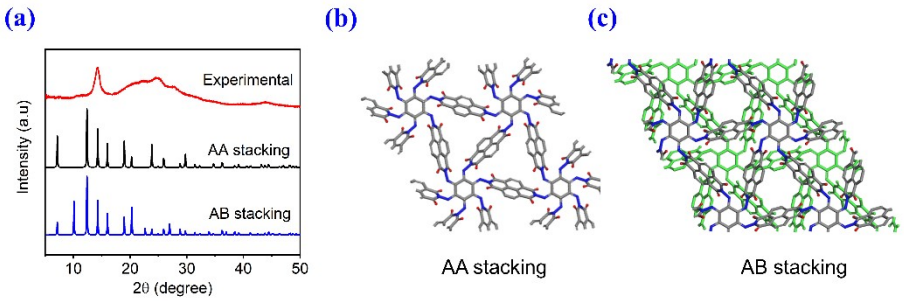

Figure S2. (a) PXRD patterns of PNDI-COF: experimental (red), simulated for AA (black), and AB (blue) stacking models. (b) Simulated structure of PNDI-COF from the AA and AB stacking model.

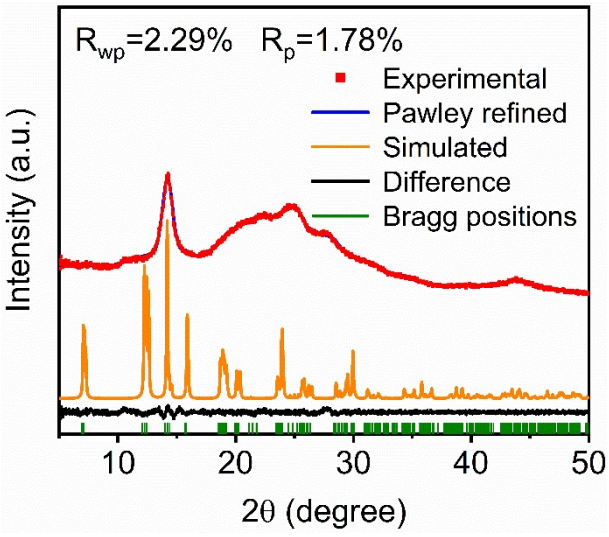

Figure S3. Pawley refinement of PNDI-COF

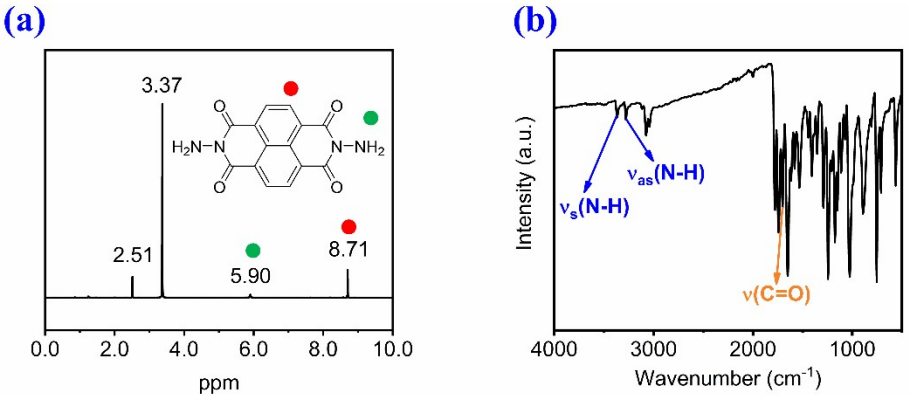

Figure S4. (a) ^{1}H NMR and (b) FT-IR spectra of NDI-NH_2.

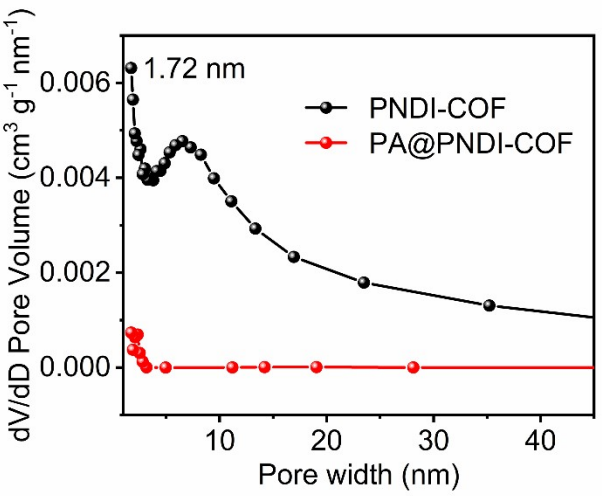

Figure S5. The pore size distribution curves of PNDI-COF and PA@PNDI-COF

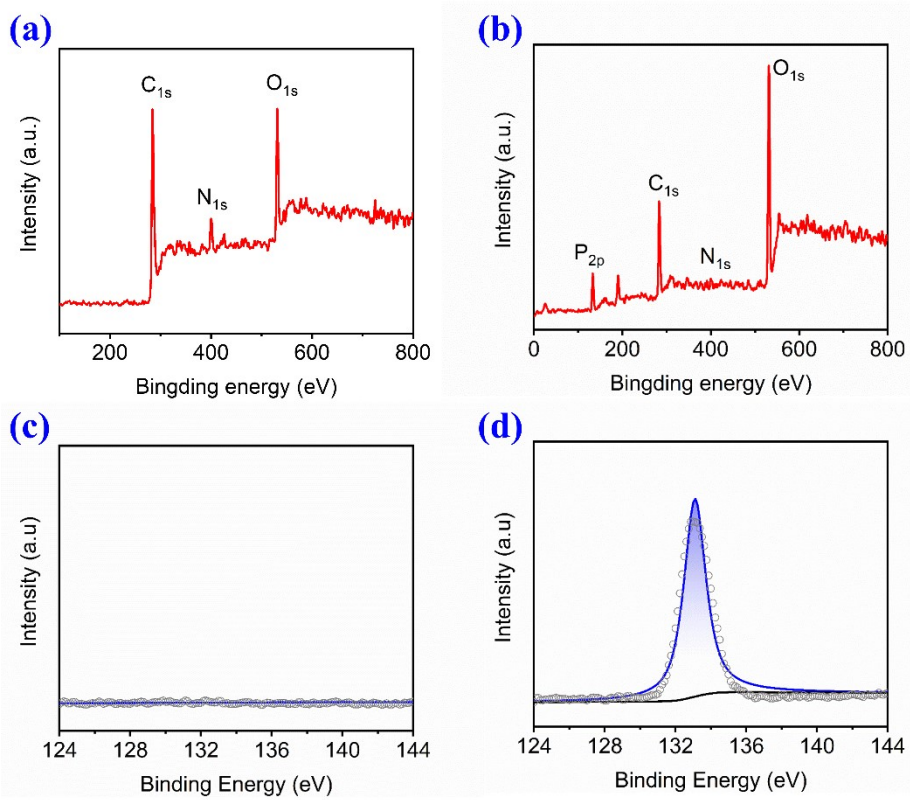

Figure S6. XPS full survey spectra (a, b) and P2p spectra (c, d) for PNDI-COF (left) and PA@PNDI-COF (right).

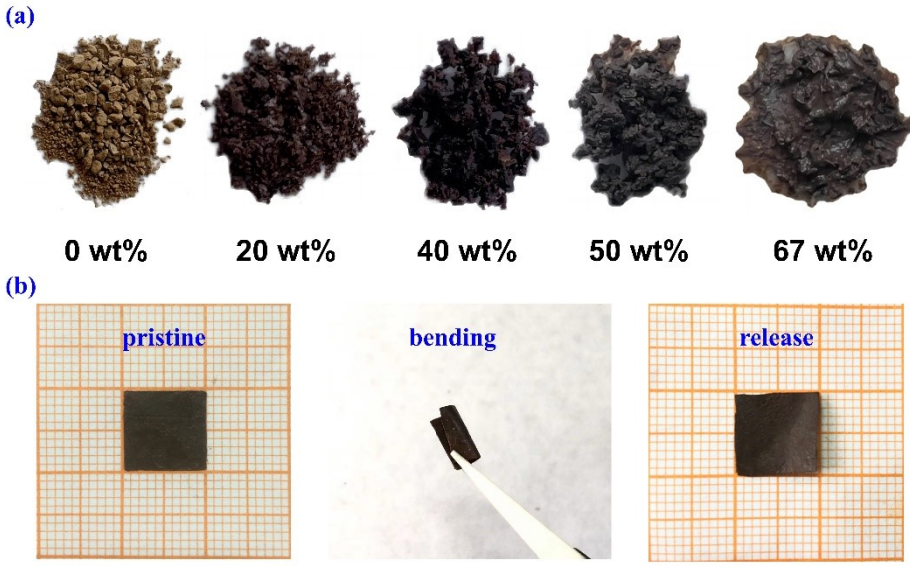

Figure S7. Photographs of (a) PA@PNDI-COF-X (X = 0−67 wt%) and (b) PA@PNDI-COF/PTFE membrane showing the flexibility.

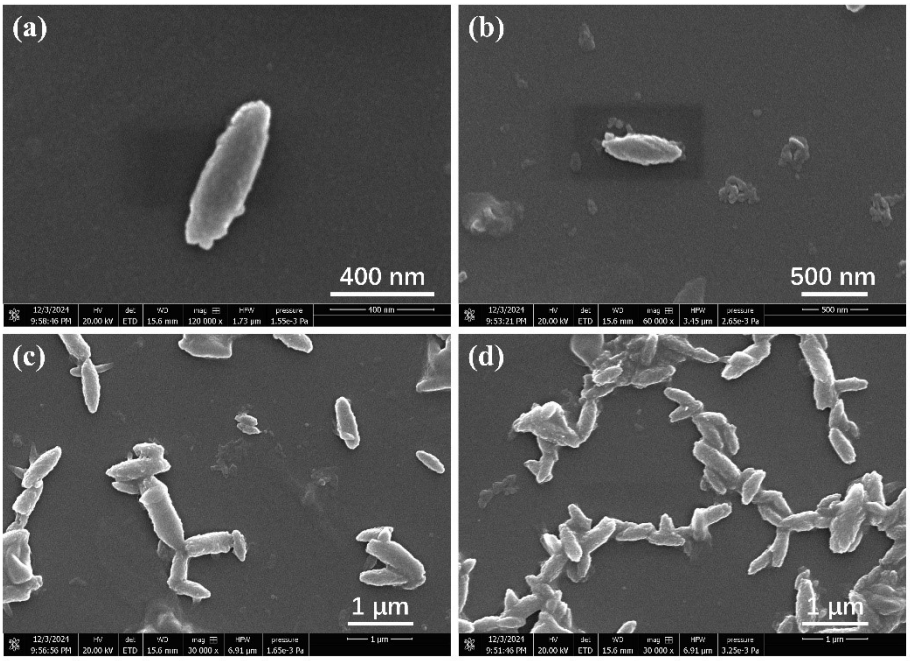

Figure S8. SEM images of PNDI-COF

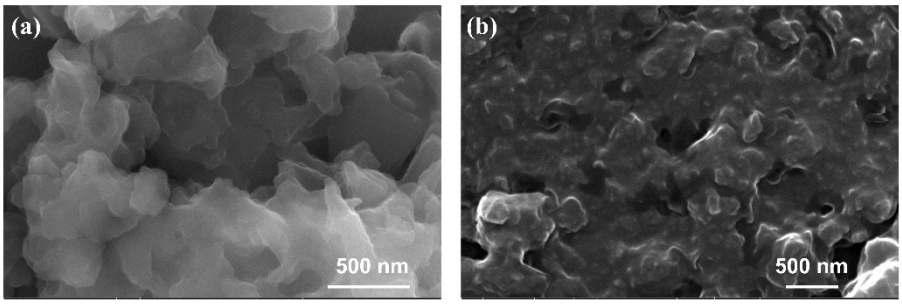

Figure S9. SEM images of PNDI-COF and PA@PNDI-COF.

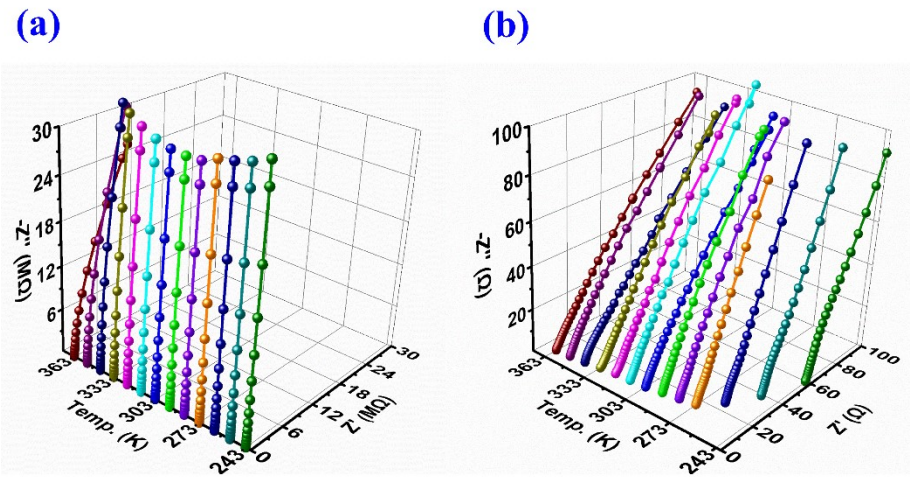

Figure S10. Temperature-dependent Nyquist plots of (a) PNDI-COF and (b) PA@PNDI-COF (−30 to 90 °C, ambient humidity).

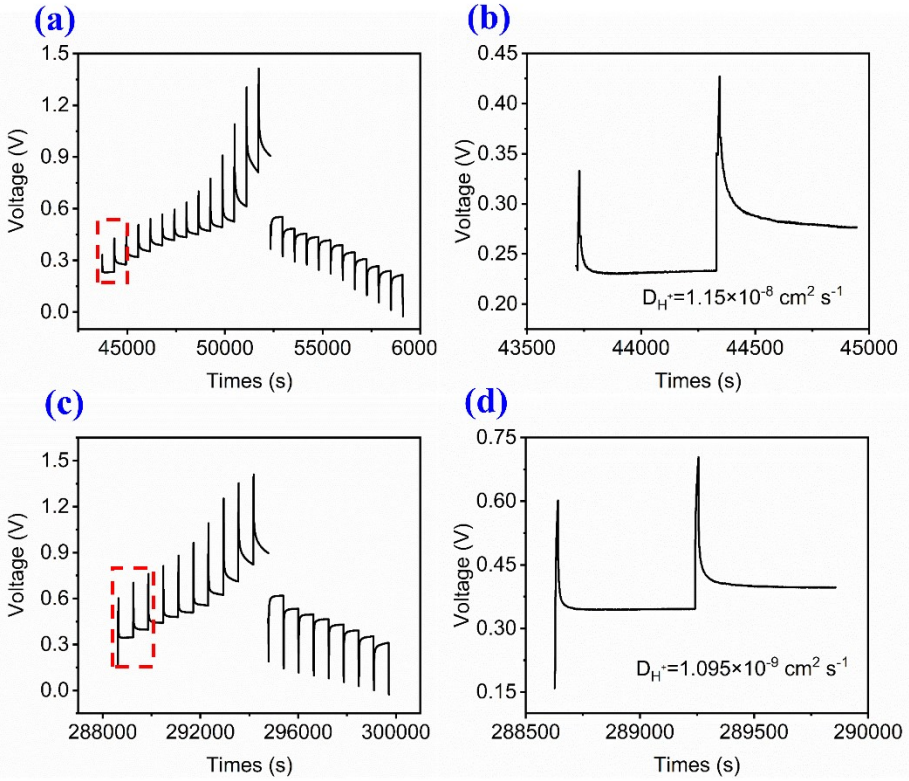

Figure S11. The GITT profiles and the selected steps of the GITT curves for full battery with different electrolytes of (a, b) PA@PNDI-COF and (c, d) 1 M H_2SO_4.

The ions diffusion coefficient (D) is calculated by galvanostatic intermittent titration technique (GITT) measurement, which follows the equation:

$$D = \frac{4L^2}{\pi\tau}\left(\frac{\Delta E_s}{\Delta E_t}\right)^2$$

Where τ is the relaxation time. ΔEs is the steady-state voltage change after current pulse. ΔEt is the voltage change (V) during the relaxation process. L is ion diffusion length (cm), which is approximately equal to the thickness of electrode.

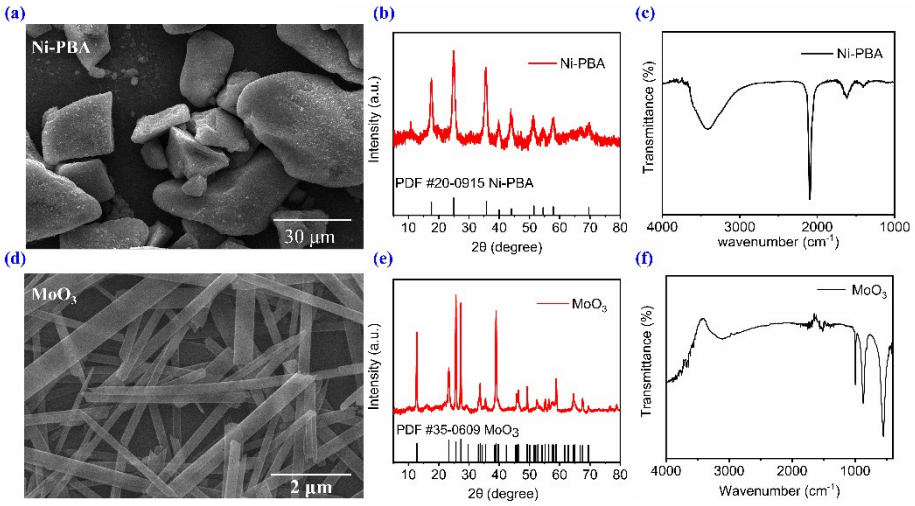

Figure S12. SEM images (a, d), PXRD patterns (b, e) and FT-IR spectra (c, f) for Ni-PBA and MoO_3. Ni-PBA was prepared by a precipitation reaction in an aqueous solution, the intense diffraction peaks in PXRD pattern of Ni-PBA, appeared in the 2θ range of 5–50°, correspond to the (2 0 0), (2 2 0), (4 0 0), (4 4 0) and (6 2 0) crystallographic plane reflections, and are good consistent with the standard PXRD card (JCPDS no. 20-0915). The intense band at 2088 cm^{-1} in FT-IR spectrum is the characteristic band of ν(C≡N) related to cyanide-coordinated Fe^{2+}, the vibration band at 3375 cm^{-1} arises from H–O stretching of interstitial water in Ni-PBA. The MoO_3 was synthesized via a modified hydrothermal method, the as-prepared nanobelt MoO_3 has a stable layered orthorhombic structure according to PXRD card (JCPDS no. 35-0609). The band at 996 cm^{-1} in FT-IR spectrum of nanobelt MoO_3 was associated with the terminal ν(Mo = O), which was an indication of layered MoO_3 phase. The bands at 867 cm^{-1} and 558 cm^{-1} are assigned to the Mo^{6+} stretching vibrations and bending vibrations of the Mo-O-Mo units.

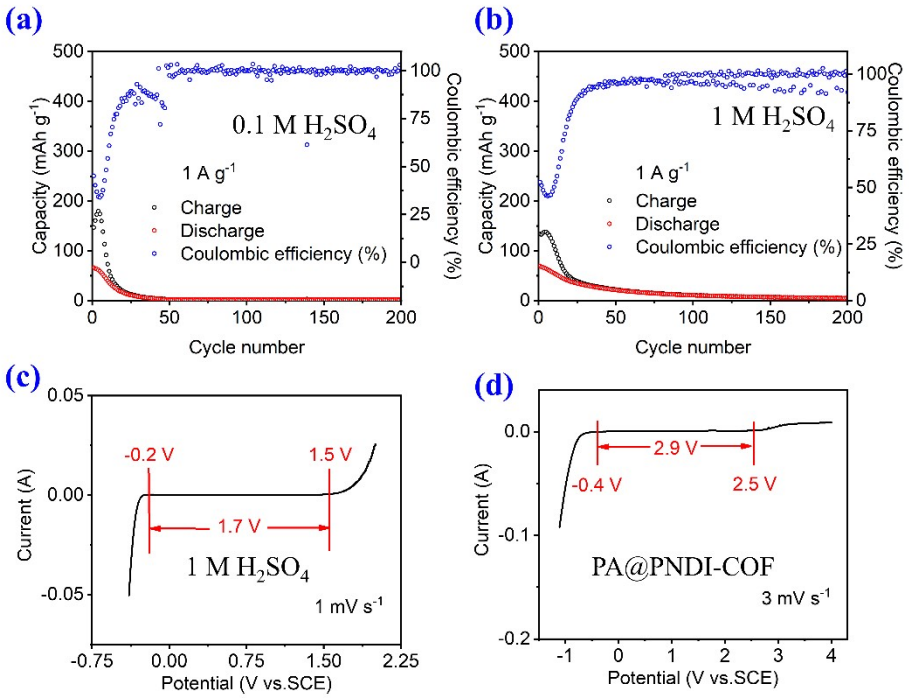

Figure S13. Cycling and Coulombic performance of full proton battery at a current of 1 A g^{-1} with (a) 0.1 M H_2SO_4 and (b) 1 M H_2SO_4 electrolyte. LSV curves of (c) 1 M H_2SO_4 and (d) PA@PNDI-COF.

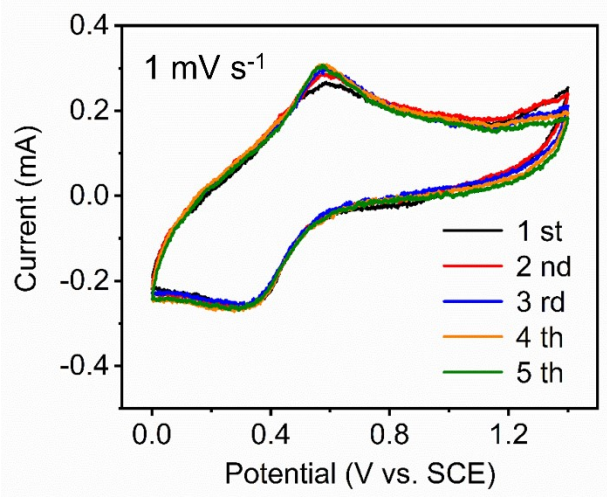

Figure S14. CV curves of full proton battery with PA@PNDI-COF electrolyte at 1 mV S^{-1}.

Table S1. Unit cell parameters of PNDI-COF from the DFT calculation.

Space group	P 1
a/Å	14.3135
b/Å	14.2454
c/Å	6.1997
α/°	90.0000
β/°	90.0000
γ/°	120.0000

Table S2. Proton conduction of PA@PNDI-COF in comparison with other high-performing COF-based proton conductors

Materials	Conductivity (mS cm^{-1})	Conditions	Ref
NKCOF-2	2.42	25 ℃ and 100% RH	**4**
TFPPY-BT-COF-H_2PO_3	0.64	20 ℃ and 98% RH	**5**
COF-HNU9	1.56	25 ℃ and 98% RH	**6**
BIY-COF	19	95 ℃ and 95% RH	**7**
TpBth	0.21	30 ℃ and 98% RH	**8**
S-COF-2	15	25 ℃ and 95% RH	**9**
trz@XJCOF-2	6.91	120 ℃ and anhydrous	**10**
$CuCl_2$@TpTta-10	8.81	100 ℃ and 98% RH	**11**
$H_2PO_4^-$@CCOF	5.28	30 ℃ and 98% RH	**12**
PIL-TB-COF	2.21	120 ℃ and anhydrous	**13**
Im@DaTta	9.1	100 ℃ and 98% RH	**14**
H_3PO_4@NKCOF-54	23.3	160 ℃ and anhydrous	**15**
TPB-DPPA-COF	0.496	90 ℃ and 98% RH	**16**
PA@PNDI-COF	18.7 38.2	20 ℃ and 25% RH 90 ℃ and 25% RH	**This work**

Reference

1 H. Langhals, A. Hofer, *J. Org. Chem.* **2013**, *78*, 5889-5897.

2 H. Jiang, W. Shin, L. Ma, J. J. Hong, Z. Wei, Y. Liu, S. Zhang, X. Wu, Y. Xu, Q. Guo, M. A. Subramanian, W. F. Stickle, T. Wu, J. Lu, X. Ji, *Adv. Energy Mater.* **2020**, *10*, 2000968.

3 Y. Yuan, D. Bin, X. Dong, Y. Wang, C. Wang, Y. Xia, *ACS Sustain. Chem. Eng.* **2020**, *8*, 3655-3663.

4 Y. Yang, P. Zhang, L. Hao, P. Cheng, Y. Chen, Z. Zhang, *Angew. Chem., Int. Ed.* **2021**, *60*, 21838-21845.

5 Z. Lu, C. Yang, L. He, J. Hong, C. Huang, T. Wu, X. Wang, Z. Wu, X. Liu, Z. Miao, B. Zeng, Y. Xu, C. Yuan, L. Dai, *J. Am. Chem. Soc.* **2022**, *144*, 9624-9633.

6 Y. Chen, J. Qiu, X.-G. Zhang, H. Wang, W. Yao, Z. Li, Q. Xia, G. Zhu, J. Wang, *Chem. Sci.* **2022**, *13*, 5964-5972.

7 S. Yang, C. Yang, C. Dun, H. Mao, R. S. H. Khoo, L. M. Klivansky, J. A. Reimer, J. J. Urban, J. Zhang, Y. Liu, *J. Am. Chem. Soc.* **2022**, *144*, 9827-9835.

8 S.-L. Zhang, Z.-C. Guo, K. Xu, Z. Li, G. Li, *ACS Appl. Mater. Interfaces* **2023**, *15*, 33148-33158.
9 L. Zhai, Y. Yao, B. Ma, M. M. Hasan, Y. Han, L. Mi, Y. Nagao, Z. Li, *Macromol. Rapid Commun.* **2022**, *43*, 2100590.
10 Y. Fu, Y. Wu, S. Chen, W. Zhang, Y. Zhang, T. Yan, B. Yang, H. Ma, *ACS Nano* **2021**, *15*, 19743-19755.
11 Z.-C. Guo, M.-L. You, Z.-J. Wang, Z.-F. Li, G. Li, *ACS Appl. Mater. Interfaces* **2022**, *14*, 15687-15696.
12 X.-F. Liu, S.-Z. Huang, Y.-X. Lian, X.-Y. Dong, S.-Q. Zang, *Chem. Commun.* **2022**, *58*, 6084-6087.
13 Y. Guo, X. Zou, W. Li, Y. Hu, Z. Jin, Z. Sun, S. Gong, S. Guo, F. Yan, *J. Mater. Chem. A* **2022**, *10*, 6499-6507.
14 S.-L. Zhang, Z.-C. Guo, A.-R. Su, J. Yang, Z.-F. Li, Y.-B. Si, G. Li, *CHEM-EUR J* **2023**, *29*, e202302146.
15 L. Hao, S. Jia, X. Qiao, E. Lin, Y. Yang, Y. Chen, P. Cheng, Z. Zhang, *Angew. Chem., Int. Ed.* **2023**, *62*, e202217240.
16 S. Wang, X. Tang, K. Yang, B. Chen, K. Zhang, H. Xu, W. Wang, G. Zhang, C. Gu, *Macromol. Rapid Commun.* **2023**, *44*, 2200678.